

TOPress3D: 3D topology optimization with design-dependent pressure loads in MATLAB

Prabhat Kumar¹

Department of Mechanical and Aerospace Engineering, Indian Institute of Technology Hyderabad, 502285, India

Abstract: This paper introduces “TOPress3D,” a 3D topology optimization MATLAB code for structures subjected to design-dependent pressure loads. With a primary focus on pedagogical objectives, the code provides an easy learning experience, making it a valuable tool and practical gateway for newcomers, students, and researchers towards this topic. TOPress3D uses Darcy’s law with a drainage term to link the given pressure load to design variables, which is converted to consistent nodal loads. Compliance minimization subjected to volume constraint optimization problems with pressure loads are solved. Load sensitivities arising due to design-dependent nature of the loads are evaluated using the adjoint-variable approach. The method of moving asymptotes is used to update the design variables. TOPress3D is constituted by six main parts. Each is described in detail. The code is also tailored to solve different problems. The robustness and success of the code are demonstrated while designing a few pressure load-bearing structures. The code is provided in Appendix B and is available with extensions in the supplementary material and publicly at <https://github.com/PrabhatIn/TOPress3D>.

Keywords: Topology optimization, Design-dependent pressure loads, MATLAB code, 3D compliance minimization problems

1 Introduction

This paper introduces “TOPress3D,” a MATLAB code (160-line) designed for performing 3D topology optimization on structures subjected to design-dependent fluidic pressure loads. While such loads are prevalent in various applications, addressing them within a topology optimization framework presents distinct challenges as they change direction, location and/or magnitude with design evolution (Hammer and Olhoff, 2000; Kumar et al., 2020). These challenges become more pronounced for 3D problems (Kumar and Langelaar, 2021). Therefore, availability of a publicly accessible pedagogical code can become particularly valuable and can serve as an educational tool and practical entry point for newcomers, students, and researchers looking to familiarize themselves with this subject. TOPress3D is developed to fill the gap and accomplish the above mentioned objectives.

These days, topology optimization (TO) has become a widely used technique in various applications, as it provides efficient and innovative optimized designs. The technique solves the associated boundary value problems typically using finite element methods, wherein the design domain is discretized by finite elements (FEs), ranging from simple elements such as triangles, quadrilaterals (Sigmund, 2001), and hexahedral elements (Amir et al., 2014; Liu and Tovar, 2014) to more advanced ones like honeycomb tessellations (Saxena, 2011; Kumar, 2023), polygonal elements (Talischi et al., 2012), and truncated octahedral elements (Chi et al., 2020; Singh et al., 2024). A design variable $\rho \in [0, 1]$ is assigned to each element that determines its state. $\rho = 0$ indicates void phase, whereas $\rho = 1$ denotes solid phase of the element. Depending on the nature of the loads, TO approaches can be classified into those with and without design-dependent loads. While many TO approaches exist for the latter, only a few

¹pkumar@mae.iith.ac.in

methods have been reported for the former (Picelli et al., 2019; Kumar et al., 2020). The number of methods further reduces when considering 3D settings (Kumar and Langelaar, 2021). One may find 3D approaches only in Du and Olhoff (2004); Zhang et al. (2010); Yang et al. (2005); Sigmund and Clausen (2007); Wang and Qian (2020); Kumar and Langelaar (2021). In addition, a 3D paper with related code does not exist yet. Therefore, the current endeavor aims to potentially eliminate barriers hindering the learning and development of 3D TO with design-dependent loads and their extensions for solving different applications experiencing such loads, e.g., pneumatically actuated soft grippers (Pinski et al., 2023, 2024), pressure-loaded meta-materials, to name a few.

Making publicly available education codes in TO is a welcomed trend, which helps the technique grow faster and provides valuable tools. This trend is well accepted in academia and industry, which was started by Sigmund while presenting the first TO educational code having 99-line in MATLAB (Sigmund, 2001). Following the trend, many 2D educational papers with codes have been presented for different applications. A list of such codes can be found in Wang et al. (2021). On the other hand, the number of 3D TO papers with code is few, e.g., in Liu and Tovar (2014); Amir et al. (2014); Amir (2015); Aage et al. (2015); Lagaros et al. (2019); Chi et al. (2020); Ferrari and Sigmund (2020); Schmidt and Schulz (2011); Deng et al. (2021); Zuo and Xie (2015); Fernández et al. (2019); Smith and Norato (2020); Wang and Kang (2021); Du et al. (2022); Zhao et al. (2023); Zhuang et al. (2023); Kim et al. (2022). In addition, one cannot find such a publicly available code for 3D TO with design-dependent pressure loads. The motif herein is to fill the gap, benefiting students, researchers, and practitioners to delve into TO with design-dependent loads and use and extend the provided code (**TOPress3D**) for different applications.

TOPress3D employs 3D hexahedral elements to parameterize design domains. It incorporates the 3D version of the Darcy law, including the drainage term described in Kumar and Langelaar (2021), to establish a relationship between the given pressure load and design variables. The 2D counterpart of this relationship is available in Kumar et al. (2020) and related MATLAB code in Kumar (2023). The variable naming conventions and framework within **TOPress3D** follow **TOPress** (Kumar, 2023). The method of moving asymptotes (MMA, cf. Svanberg (1987)) is utilized for updating the design variables in the optimization process. MMA readily permits the code extension with additional physical and/or geometrical constraints, if any. The assembly process mentioned in Ferrari and Sigmund (2020) is used for handling the symmetric matrices (stiffness and flow matrices) of **TOPress3D** for efficiency. Whereas, noting that the transformation matrix (Sec. 2) is independent of the design variables, is assembled only once before the optimization and used within the optimization process that helps cut the computational cost and requirements.

The remainder of the paper is organized as follows. Sec. 2 presents topology optimization framework—pressure field evaluation, consistent nodal load calculation, and optimization problem formulation with sensitivity analysis. Sec. 3 outlines MATLAB implementation of **TOPress3D** in detail and provides various extensions. The numerical results for loadbearing structures are presented in Sec. 4. Lastly, Sec. 5 outlines the concluding remarks.

2 Topology optimization framework

For completeness, this section briefly outlines pressure load modeling, nodal load evaluation, and nomenclature/parameters' values used in the code. Additionally, it mentions the objective formulation and sensitivity analysis for a compliance problem with a volume constraint. Readers are referred to Kumar and Langelaar (2021) for a more detailed description.

2.1 Pressure field evaluation

According to Kumar et al. (2020), Darcy’s law with a drainage term provides an elegant approach to model pressure load in a TO framework. The method has been successfully utilized to solve various problems, including 3D structures and compliant mechanism problems (Kumar and Langelaar, 2021), length-scale informed pressure-actuated compliant mechanisms (Kumar and Langelaar, 2022), a PneuNet of a soft robot (Kumar, 2022), with a featured-based method to obtain close to 0-1 topologies (Kumar and Saxena, 2022), multi-material grippers (Pinsker et al., 2023, 2024), multi-material frequency-constrained TO with polygonal FEs (Banh et al., 2024), multi-material structures with honeycomb tessellations (Kumar, 2024 (accepted)) and multi-material pneumatically driven compliant mechanisms, and 2D structures subjected to design-dependent pressure loads with MATLAB code, **TOPress** Kumar (2023) and pneumatically actuated soft robots written in MATLAB Kumar (2024). The material states of elements change as TO progresses, i.e., one can consider characteristics of elements like porous media at the beginning with known pressure differences. To this end, Darcy’s flux \mathbf{q} is defined as (Kumar et al., 2020)

$$\mathbf{q} = -\frac{\kappa}{\mu}\nabla p = -K(\tilde{\boldsymbol{\rho}})\nabla p, \quad (1)$$

where ∇p , κ , and μ indicate the pressure gradient, permeability of the medium, and the fluid viscosity, respectively. $\tilde{\boldsymbol{\rho}}$ represents the physical design vector. It is also the filtered design vector (Bruns and Tortorelli, 2001) corresponding to the design vector $\boldsymbol{\rho}$ herein. $K(\tilde{\boldsymbol{\rho}})$, flow coefficient, is defined in terms of $\tilde{\boldsymbol{\rho}}$; thus, $\boldsymbol{\rho}$, to relate the pressure field to the design vector. Mathematically, $K(\tilde{\boldsymbol{\rho}})$ for element e is written as

$$K(\tilde{\rho}_e) = K_v (1 - (1 - \epsilon)\mathcal{H}(\tilde{\rho}_e, \beta_\kappa, \eta_\kappa)), \quad (2)$$

where $\epsilon = \frac{K_s}{K_v}$ represents the flow contrast. K_v and K_s indicate the flow coefficients of void and solid phases of an element, respectively.

$$\mathcal{H}(\tilde{\rho}_e, \beta_\kappa, \eta_\kappa) = \frac{\tanh(\beta_\kappa \eta_\kappa) + \tanh(\beta_\kappa(\tilde{\rho}_e - \eta_\kappa))}{\tanh(\beta_\kappa \eta_\kappa) + \tanh(\beta_\kappa(1 - \eta_\kappa))}, \quad (3)$$

is a smooth Heaviside function. We write $\{\eta_\kappa, \beta_\kappa\}$ the flow parameters (Kumar, 2023), where η_κ and β_κ indicate the step position and slope of $K(\tilde{\rho}_e)$, respectively. We set $K_v = 1$, and $\epsilon = 1 \times 10^{-7}$, i.e., $K_s = \epsilon$ in **TOPress3D** code.

$$K(\tilde{\rho}_e) = 1 - (1 - \epsilon)\mathcal{H}(\tilde{\rho}_e, \beta_\kappa, \eta_\kappa). \quad (4)$$

The equilibrium equation corresponding to (1) is (Kumar et al., 2020)

$$\nabla \cdot \mathbf{q} = -\nabla \cdot (K(\tilde{\boldsymbol{\rho}})\nabla p) = 0 \quad (5)$$

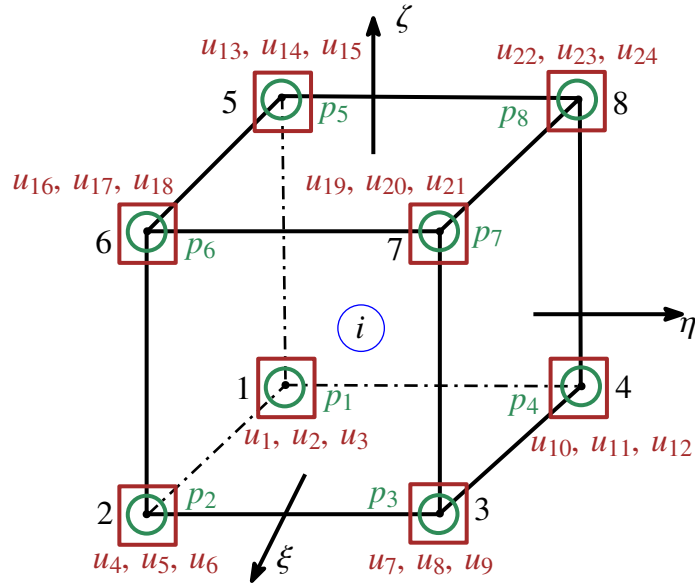
A drainage term included to achieve a realistic pressure field (Kumar and Langelaar, 2021), Eq. 5 transpires to

$$\nabla \cdot \mathbf{q} - Q_{\text{drain}} = \nabla \cdot (K(\tilde{\boldsymbol{\rho}})\nabla p) + Q_{\text{drain}} = 0. \quad (6)$$

with $Q_{\text{drain}} = -D(\tilde{\rho}_e)(p - p_{\text{ext}})$, where $D(\tilde{\rho}_e) = D_s \mathcal{H}(\tilde{\rho}_e, \beta_d, \eta_d)$. $\{\eta_d, \beta_d\}$, termed the drainage parameters, are analogous to $\{\eta_\kappa, \beta_\kappa\}$. To restrict the user-defined parameters, **TOPress3D** code considers $\eta_d = \eta_\kappa = \eta_f$ and $\beta_d = \beta_\kappa = \beta_f$. However, users are free to select as per the recommendation provided in Kumar et al. (2020).

$$D_s = \left(\frac{\ln r}{\Delta s}\right)^2 K_s, \text{ with } r = \frac{p|_{\Delta s}}{p_{\text{in}}}, \quad (7)$$

where Δs , a penetration parameter, is set equal to size of a few FEs. $p|_{\Delta s}$ indicates the pressure at Δs . One can use $r \in [0.001 \ 0.1]$ (Kumar, 2023).



- ① Element i with design variable ρ_i
- Nodes ($k = 1, \dots, 8$)
- Pressure DOFs (p_k)
- Displacement DOFs ($u_{3k-2}, u_{3k-1}, u_{3k}$)

Figure 1: Element i nomenclature. **Lface**, **Rface**, **BTface**, **Tface**, **Fface** and **Bface** represent left, right, bottom, top, front, and back faces, respectively. Herein, these faces respectively contain $\{1, 2, 5, 6\}$, $\{3, 4, 7, 8\}$, $\{1, 2, 3, 4\}$, $\{5, 6, 7, 8\}$, $\{2, 3, 6, 7\}$ and $\{1, 4, 5, 8\}$ nodes.

As mentioned, the code uses hexahedral elements (Fig. 1) to describe the design domain. A hexahedral element with node numbers is displayed in Fig. 1. With standard finite element method (FEM), Eq. 6 is written as (Kumar and Langelaar, 2021)

$$\left[\int_{\Omega_e} \left(K \mathbf{B}_p^T \mathbf{B}_p \right) dV + \int_{\Omega_e} \left(D \mathbf{N}_p^T \mathbf{N}_p \right) dV \right] \mathbf{p}_e = \mathbf{0}, \quad (8)$$

while considering $p_{\text{out}} = 0$ and $\mathbf{q}_\Gamma = 0$. $\mathbf{N}_p = [N_1, N_2, N_3, \dots, N_8]$ are the trilinear shape functions (Appendix A) for the hexahedral elements (Fig. 1), $\mathbf{B}_p^T = \nabla \mathbf{N}_p$, and $\mathbf{p}_e = [p_1, p_2, p_3, \dots, p_8]^T$. Note N_k and p_k ($k = 1, \dots, 8$) indicate shape function and pressure degree of freedom for the k^{th} node of hexahedral element i , respectively (Fig. 1). To this end, Eq. (8) yields to

$$\mathbf{K}_p^e \mathbf{p}_e + \mathbf{K}_{Dp}^e \mathbf{p}_e = \mathbf{A}_e \mathbf{p}_e = \mathbf{0}, \quad (9)$$

where element flow matrices of the Darcy and drainage parts are \mathbf{K}_p^e and \mathbf{K}_{Dp}^e , respectively. They are evaluated and their numerical value are provided in Appendix A. $\mathbf{A}_e = \mathbf{K}_p^e + \mathbf{K}_{Dp}^e$ is the overall element flow matrix. Upon assembly, (9) yields to

$$\mathbf{A} \mathbf{p} = \mathbf{0}, \quad (10)$$

\mathbf{K}_p^e and \mathbf{K}_{Dp}^e are symmetric matrices; thus, \mathbf{A} is a symmetric matrix. Eq. 10 is solved while applying the given pressure load boundary conditions. \mathbf{A} and \mathbf{p} are sub-blocked into free and prescribed, denoted using subscripts f and p , respectively; Eq. 10 is rewritten as (Kumar, 2024)

$$\begin{bmatrix} \mathbf{A}_{ff} & \mathbf{A}_{fp} \\ \mathbf{A}_{fp}^T & \mathbf{A}_{pp} \end{bmatrix} \begin{bmatrix} \mathbf{p}_f \\ \mathbf{p}_p \end{bmatrix} = \begin{bmatrix} \mathbf{0} \\ \mathbf{0} \end{bmatrix} \quad (11)$$

$\mathbf{p}_f = \mathbf{A}_{ff}^{-1} \mathbf{A}_{fp} \mathbf{p}_p$; i.e., one gets the pressure field \mathbf{p} as a function of physical variables (design variables).

2.2 Nodal load evaluation

The pressure field \mathbf{p} is transformed into nodal loads by applying equilibrium conditions on an elemental cube experiencing body forces (Kumar et al., 2020; Kumar and Langelaar, 2021). We get (Kumar et al., 2020)

$$\mathbf{b}dV = -\nabla p dV, \quad (12)$$

where dV and \mathbf{b} indicate elemental volume and body force per unit volume, respectively. Given standard FEM, the nodal force \mathbf{F}_e for an element is determined as (Kumar and Langelaar, 2021)

$$\begin{aligned} \mathbf{F}_e &= \int_{\Omega_e} \mathbf{N}_u^\top \mathbf{b} dV = - \int_{\Omega_e} \mathbf{N}_u^\top \nabla p dV \\ &= - \left[\int_{\Omega_e} \mathbf{N}_u^\top \mathbf{B}_p dV \right] \mathbf{p}_e = \mathbf{T}_e \mathbf{p}_e, \end{aligned} \quad (13)$$

where $\mathbf{N}_u = [N_1 \mathbf{I}, N_2 \mathbf{I}, N_3 \mathbf{I}, \dots, N_8 \mathbf{I}]$, with \mathbf{I} the identity matrix in \mathcal{R}^3 . \mathbf{F}_e is assembled to achieve its global nodal force vector \mathbf{F} . Expression and numerical value for \mathbf{T}_e are provided in Appendix A. Eq. (12) transpires to

$$\mathbf{F} = -\mathbf{T}\mathbf{p}, \quad (14)$$

in the global sense. \mathbf{T} is the global transformation matrix. Note that \mathbf{T}_e is independent of design variables; thus, it is assembled prior to the optimization steps to determine \mathbf{T} . This step helps save computational requirements; thus, making code relatively efficient.

2.3 Objective and sensitivity analysis

We solve the following optimization problem for the three-dimensional loadbearing structures with a given volume constraint:

$$\left. \begin{aligned} \min_{\tilde{\boldsymbol{\rho}}} \quad & C(\tilde{\boldsymbol{\rho}}) = \mathbf{u}^\top \mathbf{K}(\tilde{\boldsymbol{\rho}}) \mathbf{u} = \sum_{j=1}^{nel} \mathbf{u}_j^\top \mathbf{k}_j(\tilde{\rho}_j) \mathbf{u}_j \\ \text{subjected to:} \quad & \lambda_1 : \mathbf{A}\mathbf{p} = \mathbf{0} \\ & \lambda_2 : \mathbf{K}\mathbf{u} = \mathbf{F} = -\mathbf{T}\mathbf{p} \\ & \Lambda : V(\tilde{\boldsymbol{\rho}}) - V^* \leq 0 \\ & \mathbf{0} \leq \tilde{\boldsymbol{\rho}} \leq \mathbf{1} \\ \text{Data:} \quad & V^*, E_0, E_{\min}, p, K_v, \epsilon, \eta_f, \beta_f \end{aligned} \right\}, \quad (15)$$

where C and nel denote the structure's compliance and total number of elements used to represent design domain (Ω_e). \mathbf{K} is the global stiffness matrix, whereas \mathbf{u} indicates the global displacement vector. \mathbf{k}_j and \mathbf{u}_j are stiffness matrix and displacement vector for element j , respectively. V^* and V denote the permitted and current volume of Ω_e , respectively. \mathbf{F} indicates the global force vector. λ_1 , λ_2 and Λ are the Lagrange multipliers. The former two are vectors, whereas the latter one is a scalar. Vector $\tilde{\boldsymbol{\rho}}$ represent filtered counterparts of design variable vector $\boldsymbol{\rho}$. The first vector is termed the physical vector herein.

One determines filtered design variable for element i as:

$$\tilde{\rho}_i = \frac{\sum_{j=1}^{nel} \rho_j v_j w(\mathbf{x}_i, \mathbf{x}_j)}{\sum_{j=1}^{nel} v_j w(\mathbf{x}_i, \mathbf{x}_j)}, \quad (16)$$

where $w(\mathbf{x}_i, \mathbf{x}_j) = \max\left(0, 1 - \frac{\|\mathbf{x}_i - \mathbf{x}_j\|}{r_{\text{fill}}}\right)$ (Bruns and Tortorelli, 2001), r_{fill} and v_j are filter radius and volume of element j , respectively. One can determine v_j and $w(\mathbf{x}_i, \mathbf{x}_j)$ prior to the optimization and can store in a matrix \mathbf{H} as:

$$H_{i,j} = \frac{v_j w(\mathbf{x}_i, \mathbf{x}_j)}{\sum_{j=1}^{\text{nel}} v_j w(\mathbf{x}_k, \mathbf{x}_j)}. \quad (17)$$

The filtered design vector and its derivative with respect to the design vector can be written as $\tilde{\boldsymbol{\rho}} = \mathbf{H}\boldsymbol{\rho}$ and $\frac{\partial \tilde{\boldsymbol{\rho}}}{\partial \boldsymbol{\rho}} = \mathbf{H}^\top$, respectively. T0Press3D uses `imfilter` MATLAB function for the filtering operations (see Appendix B).

The modified Solid Isotropic Material with Penalization (SIMP) interpolation scheme is used. Young's modulus of element i , E_i , is written as

$$E_i = E_{\min} + \tilde{\rho}_i^p (E_1 - E_{\min}), \quad (18)$$

where p is the SIMP parameter. E_1 and E_{\min} are Young's moduli of element's solid and void states, respectively.

2.3.1 Sensitivity analysis

We use the method of moving asymptotes (MMA, cf. Svanberg (1987)), a gradient-based optimizer, for updating the design variables. Thus, we need objective's and constraint's derivatives with respect to the design variables, which are determined using the adjoint-variable method herein. The augmented performance function \mathcal{L} in terms of objective function and equilibrium equations (15) can be written as (Kumar, 2023)

$$\mathcal{L} = \mathbf{u}^\top \mathbf{K} \mathbf{u} + \boldsymbol{\lambda}_1^\top \mathbf{A} \mathbf{p} + \boldsymbol{\lambda}_2^\top (\mathbf{K} \mathbf{u} + \mathbf{T} \mathbf{p}). \quad (19)$$

Equation (19) is differentiated with respect to the physical design variable, and rearranging, one gets

$$\begin{aligned} \frac{d\mathcal{L}}{d\tilde{\rho}_i} = & \mathbf{u}^\top \frac{\partial \mathbf{K}}{\partial \tilde{\rho}_i} \mathbf{u} + \boldsymbol{\lambda}_2^\top \left(\frac{\partial \mathbf{K}}{\partial \tilde{\rho}_i} \mathbf{u} \right) + \boldsymbol{\lambda}_1^\top \left(\frac{\partial \mathbf{A}}{\partial \tilde{\rho}_i} \mathbf{p} \right) \\ & + \underbrace{\left(2\mathbf{u}^\top \mathbf{K} + \boldsymbol{\lambda}_2^\top \mathbf{K} \right)}_{\Xi_1} \frac{\partial \mathbf{u}}{\partial \tilde{\rho}_i} + \underbrace{\left(\boldsymbol{\lambda}_1^\top \mathbf{A} + \boldsymbol{\lambda}_2^\top \mathbf{T} \right)}_{\Xi_2} \frac{\partial \mathbf{p}}{\partial \tilde{\rho}_i} \end{aligned} \quad (20)$$

One use $\Xi_1 = 0$ and $\Xi_2 = 0$ to determine $\boldsymbol{\lambda}_1$ and $\boldsymbol{\lambda}_2$ from the above equation, i.e.,

$$\begin{aligned} \boldsymbol{\lambda}_2 &= -2\mathbf{u}, \\ \boldsymbol{\lambda}_1^\top &= -\boldsymbol{\lambda}_2^\top \mathbf{T} \mathbf{A}^{-1} = 2\mathbf{u}^\top \mathbf{T} \mathbf{A}^{-1}, \end{aligned} \quad (21)$$

and, therefore,

$$\frac{dC}{d\tilde{\rho}_i} = -\mathbf{u}^\top \frac{\partial \mathbf{K}}{\partial \tilde{\rho}_i} \mathbf{u} + \underbrace{2\mathbf{u}^\top \mathbf{T} \mathbf{A}^{-1} \frac{\partial \mathbf{A}}{\partial \tilde{\rho}_i} \mathbf{p}}_{\text{Load sensitivities}} \quad (22)$$

Load sensitivities, appeared in Eq. (22) due to the design-dependent nature of the load, affect the optimized topologies as demonstrated in prior work such as Kumar (2024); Kumar et al. (2020); Kumar (2023). Therefore, neglecting them during optimization may not be advisable. Finally, using the chain rule, the objective derivatives can be determined (Kumar, 2023). Calculation of the derivative of the volume constraint is straightforward (Sigmund, 2001). In the subsequent section, we provide the MATLAB implementation for T0Press3D code.

3 Structure of T0Press3D

The section provides a complete description of the MATLAB code, T0Press3D. Reader can download the code, provided in Appendix B, and its extensions from the supplementary material of the paper. One calls the code in the MATLAB command window as

```
T0Press3D(nelx,nely,nelz,volf,penal,rmin,etaf,betaf,lst,maxit)
```

where **nelx**, **nely** and **nelz** indicate the number of elements in x -, y - and z -directions, respectively. **volf** represents the given volume fraction, **penal** refers to the penalty parameter of the SIMP technique (Eq. 18), **rmin** is the filter radius, **etaf** and **betaf** are related to the flow coefficient and drainage term, respectively. **lst** indicates the status of load-sensitivities. **lst** = 1 indicates that load sensitivities are considered in the optimization process, whereas **lst** = 0 means otherwise. **maxit** variable indicates the maximum number of MMA iterations. Hexahedral elements are used for discretizing the domains. Local degree of freedoms (DOFs) pertaining to displacement and pressure are shown in Fig. 1. T0Press3D contains the following six main parts:

- (I) MATERIAL and FLOW PARAMETERS initialization
- (II) FINITE ELEMENT ANALYSIS and PASSIVE SOLID/VOID REGIONS preparations
- (III) Assigning PRESSURE B.Cs, DISPLACEMENT B.Cs, and LAGRANGE MULTIPLIERS initialization
- (IV) FILTER PREPARATION
- (V) MMA OPTIMIZATION PREPARATION and INITIALIZATION
- (VI) MMA OPTIMIZATION LOOP
 - (VI.1) SOLVING FLOW BALANCED EQUATION
 - (VI.2) DETERMINING CONSISTENT NODAL LOADS and GLOBAL DISPLACEMENT Vector
 - (VI.3) OBJECTIVE, CONSTRAINT and THEIR SENSITIVITIES COMPUTATION
 - (VI.4) SETTING and CALLING MMA OPTIMIZATION
 - (VI.5) PRINTING and PLOTTING RESULTS

We describe each part in detail below:

(I) **MATERIAL and FLOW PARAMETERS initialization:** **E1** (line 3) and **Emin** (line 4) indicate E_1 (Eq. 18) and E_{\min} (Eq. 18), respectively. Line 5 mentions Poisson's ratio, **nu**, which is set to 0.30. On line 6, values of K_v (Eq. 2), indicated by **Kv**, ϵ (Eq. 2), indicated by **epsf**, r and Δs , indicated by **Dels** (Eq. 7), are given utilizing **deal** MATLAB function. **deal** function creates multiple output variables with specified values. D_s and $(K_v - K_s)$ are denoted by **Ds** and **Kvs**, respectively, and are determined on line 7.

(II) **FINITE ELEMENT ANALYSIS and ACTIVE/PASSIVE REGIONS preparations:** This part provides FE analysis preparation for flow and structure parts of the code on lines 8-87. The part at end also facilitates the inclusion of passive solid/void regions, if any. Number of nodes in x -, y - and z -directions are recorded in **ndx**, **ndy** and **ndz**, respectively on line 9. **nel** and **nno** indicate the total number of FEs and nodes, respectively. **nel** and **nno** are determined on line 10. As node numbers and associated displacement and pressure DOFs are integers, we use **int32** MATLAB function while recording them. Instead of using **sparse** MATLAB function, we use **fsparse** routine, created by (Engblom and Lukarski, 2016) to perform the assembly procedure. The former records locations

(DOFs-rows and columns) information as double precision numbers, whereas the latter records them as integers, thus saving computational requirements that, in turn, make the procedure computationally efficient (Ferrari and Sigmund, 2020). Next, we mention the procedure to use/install **fsparse**.

For using **fsparse**, one can download the “**stenglib**” library² and install it as per the **README.md** file. Extract the downloaded ‘stenglib-master.zip’ file, copy the folder “Fast” and make it the current folder in MATLAB and then type ‘make’ in the command windows and press ‘Enter’ bottom on the keyboard. If MATLAB requests to install ‘MinGW64 Compiler (C)’, install the said compiler and run ‘make’ again as procedure said earlier. Once the compilation is done, the user can see the ‘MEX-file’ in the “Fast” folder. One can then place **TOPress3D.m** code with **mmasub.m** and **subsolv.m** files in ‘Fast’ folder and execute **TOPress3D.m** and its extensions.

The matrix containing displacement DOFs, recorded in **Udofs**, is created on lines 13-14 using array **nodenrs** (line 11) and vector **edofVec** (line 12). Line 15 determines pressure DOFs, all pressure DOFs, and displacement DOFs. They are recorded in **Pdofs**, **allPdofs** and **allUdofs**, respectively. Nodes constituting faces are determined next, as they are required to apply the given pressure loads. In that view, lines 16-20 determine nodes that form the bottom and top faces of domain in vectors **BTface** and **Tface**, respectively. In addition, nodes making the left and right faces are recorded on line 21 in vectors **Lface** and **Rface**, respectively. Further, line 22 determines nodes constituting the front and back faces in vectors **Fface** and **Bface**, respectively. Vectors **iK** and **jK**, required for performing assembly of the stiffness matrix, are determined on line 28 as per Ferrari and Sigmund (2020). To reduce the assembly indexing, **Iar** is determined on line 29, which is used on line 129. Lines 30-53 record the lower half of the elemental stiffness matrix in vector **Ke**. **Ke** is used for the assembling the stiffness matrix on line 129; also, to recover the complete elemental matrix **Ke0** on lines 54. **Ke0** (lines 54-56) is used to evaluate the compliance sensitivity on line 135. Following the above steps, vectors **iP** and **jP**, analogous to vectors **iK** and **jK**, are determined on line 61 for flow matrix assembly. **IarP** analogous to **Iar** is determined on line 62. Element flow matrix corresponding to the Darcy law (**Kp1**) and drainage term (**KDp1**), in the factorized form, are recorded on lines 63-64 and lines 65-66, respectively. **Kp1** and **KDp1** indicate \mathbf{K}_p^e and \mathbf{K}_{DP}^e (Eq. 9), respectively with unit K (Eq. 8) and D (Eq. 8) (see Appendix A). The corresponding full matrices **Kp** and **KDp** are recovered between lines 67-69. These matrices are needed while determining the load sensitivities (lines 136-138). Lengths of vectors **Ke** and **Kp1** are determined on line 70 utilizing, which are used later on lines 128 and line 119, respectively. On lines 71-77, the code records elemental transformation matrix **Te** (Eq. 13) in the vectorized form in vector **Te**. As **Te** is a rectangular matrix, the assembly procedure to determine the global transformation matrix **T** (Eq. 14) is similar to **TOPress** code. Vectors **iT** and **jT** are created on lines 78 and 79, respectively. Noting that the transformation matrix is independent of the design variables, the global form **T** (Eq. 14) is determined on line 81 and recorded in **TG**. This steps save computational requirements.

Smooth Heaviside projection function (Eq. 3), **IFprj**, needed to define the flow (Eq. 2) and drainage (Eq. 6) coefficients, is defined on lines 82-83. The function has three input variables. Lines 84-85 determine its derivative with respect to the first variable, i.e., the design variable, and recorded in a function **dIFprj**. The derivative function is required on lines 136-137 to determine the load sensitivities. Line 86 gives room to include passive solid (NDS)/void (NDV) regions, if any. Active design vector is determined on line 87 and is recorded in **act**.

(III) Assigning PRESSURE B.Cs and DISPLACEMENT B.Cs, and LAGRANGE MULTIPLIERS initialization: This part of the code assigns pressure load and boundary conditions, displacement boundary conditions (fixed and free DOFs). This part also initializes the global displacement and λ_1 (Eq. 21). On line 89, vector **PF** initializes pressure load vector, and scalar **Pin** contains the magnitude of the input pressure load. Line 90 updates **PF** as per the applied pressure loading locations. Fixed pressure DOFs, recorded in **fixedPdofs**, and free pressure DOFs, stored in **freePdofs**, are determined on line 91 and line 92, respectively. On line 93, array **pfixeddofsv** records the fixed pressure

²<https://github.com/stefanengblom/stenglib>

DOFs and corresponding values in its first and second columns, respectively. Lines 94-95 record fixed displacement nodes in vector `fixnn`. Vector `fixedUdofs` stores fixed displacement DOFs (line 96). Free displacement DOFs are recorded in `freeUdofs` (line 97). The global displacement vector `U` and Lagrange multiplier `lam1` for the sensitive analysis are initialized on line 98.

(IV) **FILTER PREPARATION:** `imfilter` MATLAB function is used for performing the density filtering. The filter variable `Hs` is determined on lines 99-103. One can also determine the filters parameters as (Amir et al., 2014; Amir, 2015; Liu and Tovar, 2014):

```

iH = ones(nelx*nely*nelz*(2*(ceil(rmin)-1)+1)^3,1);
jH = ones(size(iH));
sH = zeros(size(iH));
k = 0;
for i1 = 1:nelx
    for k1 = 1:nelz
        for j1 = 1:nely
            e1 = (i1-1)*nely*nelz + (k1-1)*nely + j1;
            for i2 = max(i1-(ceil(rmin)-1),1):min(i1+(ceil(rmin)-1),nelx)
                for k2 = max(k1-(ceil(rmin)-1),1):min(k1+(ceil(rmin)-1),nelz)
                    for j2 = max(j1-(ceil(rmin)-1),1):min(j1+(ceil(rmin)-1),
                        nely)
                        e2 = (i2-1)*nely*nelz + (k2-1)*nely + j2;
                        k = k + 1;
                        iH(k) = e1;
                        jH(k) = e2;
                        sH(k) = max(0,rmin-sqrt((i1-i2)^2+(j1-j2)^2+(k1-k2)^2)
                            );
                    end
                end
            end
        end
    end
end
Hk = sparse(iH,jH,sH);
Hs = sum(Hk,2);

```

and replace line 111, line 142 and line 151 (right part) by

```

dVol = Hk*(dVol0./Hs);

```

```

objsens = Hk*(objsens*normf./Hs);

```

and

```

xphys = (Hk*xphys(:))./Hs;

```

respectively.

(V) **MMA OPTIMIZATION PREPARATION and INITIALIZATION:** Lines 104-112 provide this part of the code. Line 105 initializes design variable vector `x` and provides the unfiltered derivative of the volume constraint in vector `dVol0`. `x` is updated on line 106 using the active design variable vector `act`. `nMMA`, `mMMA`, `xphys`, `xMMA`, and `mvLt` indicate the number of design variables, number of the constraints, physical design vector, design variable used in the MMA, and external move limit for the MMA, respectively. These variables are defined on line 107. Vectors `xminvec` and `xmaxvec` define the minimum and maximum value of the design vector (line 108). Lower (`low`) and upper (`upp`) values of the design vector are defined on line 109. The same line also initializes vectors `xold1` and `xold2`, which will be used to restore the old design vector during optimization. Other important parameters of the MMA, e.g., `cMMA`, `dMMA`, `a0` and `aMMA` are defined on line 110 (Svanberg, 1987). As density filtering is volume preserving, we perform filtering of the derivatives of the volume constraint above the

optimization loop on line 111 in vector `dVol`. `loop` records the optimization loop, and `change` tracks the absolute change in the design vector during optimization (line 112).

(VI) **MMA OPTIMIZATION LOOP:** The MMA optimization loop contains five parts, which starts with `while` loop with termination conditions on `maxit` and `change`. Lines 113-160 describe this part of the code. Line 114 defines the definition of the `while` loop. `loop` is used to store the progress optimization's iterations line 115.

(VI.1) **SOLVING THE FLOW BALANCE EQUATION** (Lines 116-124): This part of the code provides the pressure field in terms of the physical (design) variables. The flow coefficients (K , cf. Eq. 2) and drainage coefficients (D , cf. Eq. 6) of all FEs are recorded in vectors `Kc` (line 117) and `Dc` (line 118), respectively. The elemental flow coefficient matrix due to the Darcy law and drainage term, \mathbf{A}_e , (Eq. 9) is determined on line 119 and recorded in `Ae`. The global flow coefficient matrix, \mathbf{A} (Eq. 10), (in lower triangular form) is determined on line 120 using `fsparse` and recorded in `AG`. Line 121 determines the flow coefficient matrix corresponding to the free pressure DOFs and records in `Aff`. The full matrix of `AG` is recovered on line 122. Line 123 determines pressure field, \mathbf{p} (Eq. 10), and stores in `PF`. We use `decomposition` MATLAB function with 'ldl' type and 'lower' format for determining `PF`. Pressure load vector `PF` is modified per the known pressure load conditions on line 124.

(VI.1) **DETERMINING CONSISTENT NODAL LOAD and GLOBAL DISPLACEMENT Vectors** (Lines 125-131): Line 126 provides global load vector `F` using matrix `TG` (line 81) and vector `PF` (line 124). Young's modulus vector `E` is determined on line 127. The elemental stiffness matrix is stored in the vector form on line 128, which is further used for determining the global stiffness matrix \mathbf{K} (Eq. 15) on line 129. The latter is stored in matrix `KG`. Cholesky factorization function `chol` is used on line 130. On line 131, the global displacement vector `U` is determined. One can also replace the direct solver with the multigrid/preconditioned CG (Amir et al., 2014; Amir, 2015) to obtain vectors `PF` and `U`.

(VI.3) **OBJECTIVE, CONSTRAINT and THEIR SENSITIVITIES COMPUTATION** (Line 132-142): The objective is determined on line 133. λ_1 is determined on line 134 and stored in `lam1`. Derivatives of the objective without load sensitivity terms are determined on line 135 and are stored in `objst1`. The load sensitivities are determined on line 138 using `dc1k` (line 136, contribution from the Darcy law) and `dc1d` (line 137, contribution from the drainage term) and are stored in a vector `objst2`. The final derivatives are determined on line 139 and are recorded in `objsens`. `lst` defines presence (`lst=1`) or absence (`lst=0`) of `objst2` in vector `objsens`. On line 140, the volume fraction of the intermediate design is determined in `Vol`. Normalization parameter `normf` is defined and determined on line 141. `normf` is utilized to normalize the objective; thus, the objective derivatives consistently. The vector `objsens` is filtered while normalizing on line 142.

(VI.4) **SETTING and CALLING MMA OPTIMIZATION** (Lines 143-152): `xval` is initialized with `xMMA` on line 144. Vectors `xminvec` and `xmaxvec` are updated on line 145 using vector `xval` and parameter `mvLt`. The MMA subroutine `mmasub` is called on line 146, which updates the new design variable `xmma`. Vectors `xold1` and `xold2` are updated on line 149. A new design vector `xnew` is determined using `xmma` on line 149. `change` is determined on line 150 using the new and old design vectors. Line 150 also updates `xMMA` using `xnew`. On line 151, the physical design vector `xphys` is updated, and filtering is performed. Next line updates `xphys` using information for the solid and void passive regions.

(VI.5) **PRINTING and PLOTTING RESULTS** (Lines 153-159): We print `loop`, objective value, volume fraction, and `change` on line 154 using `fprintf` MATLAB function. MATLAB functions `cla`, `shftdim`, `smooth3`, `patch`, `view`, `axis`, `drawnow` and `camlight` functions are used

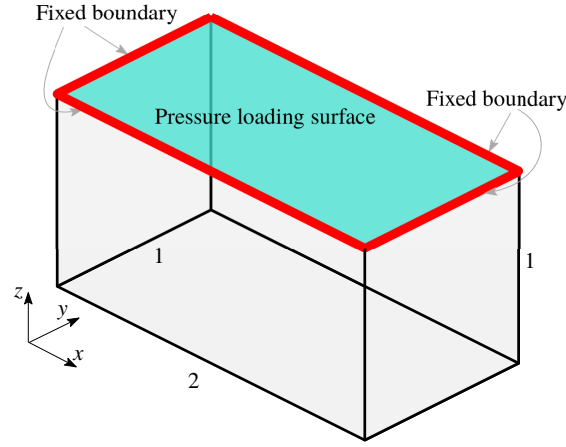


Figure 2: Design domain for a loadbearing lid structure. Pressure load is applied on the top surface, and all its edges are fixed.

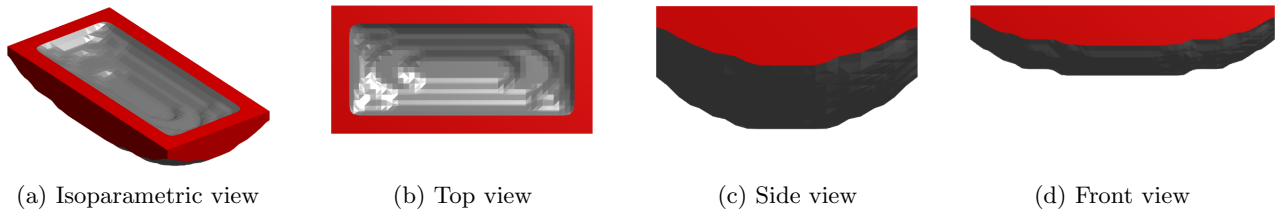


Figure 3: Optimized pressure loadbearing lid structure in different views. The domain is parameterized using $48 \times 24 \times 24$ FEs. The density value of the isosurface displayed is 0.3

to plot the optimized results (Amir et al., 2014; Amir, 2015) between lines 155-159. On line 160, the `while` loop gets ended.

4 Results

We provide four examples of pressure loadbearing structures to demonstrate the versatility and robustness of `TOPress3D`. In the material and flow definition, we set $E1 = 1$, $E_{min} = E1 \times 10^{-5}$, $\nu = 0.3$, $K_v = 1$, $\epsilon_{psf} = 10^{-7}$, $r = 0.1$, and $De1s = 2$. We use a 64-bit laptop with Processor Intel(R) Core(TM) i5-8265U 1.60 GHz, RAM 8GB, Windows 11 Pro, and MATLAB 2022a for presenting the numerical results herein.

4.1 Loadbearing Lid Structure

`TOPress3D` is the default for designing a pressure loadbearing structure for a lid design. The problem is reported earlier in Du and Olhoff (2004); Sigmund and Clausen (2007); Zhang et al. (2010); Kumar and Langelaar (2021).

The design domain, applied pressure load, and displacement boundary conditions are illustrated in Fig. 2. The top surface of the domain experiences pressure load, whereas the remaining faces receive zero pressure loading. All edges of the top surface are fixed. Dimension of the domain is considered to be $2 \times 1 \times 1$. While the problem has symmetry with respect to the vertical planes, we use the entire domain to obtain the optimized design to notice any deviation from the symmetry.

We call `TOPress3D` in the MATLAB command windows as

```
TOPress3D(48,24,24,0.25,3,sqrt(3),0.20,10,1,100);
```

wherein `nelx` = 48, `nely` = 24, `nelz` = 24, `volf` = 0.25, `rmin` = $\sqrt{3}$, `etaf` = 0.20, `betaf` = 10, `lst` = 1, `maxit` = 100. The optimized loadbearing lid structure in different views is displayed in Fig. 3. The density value of the isosurface displayed is 0.3 for the optimized design (Fig. 3). Note that to obtain the top view, side view, and front view, one changes `view(3)` (line 159) to `view(90,90)`, `view(180,0)`, and `view(90,0)`, respectively. The obtained optimized design is symmetrical and provides a suitable chamber on the top surface to contain more fluid pressure while optimizing the strength of the design. The normalized-objective and volume fraction convergence histories are depicted in Fig. 4. The convergence plots are smooth and converge close to 20th MMA iteration. The volume constraint remains active at the end of the optimization.

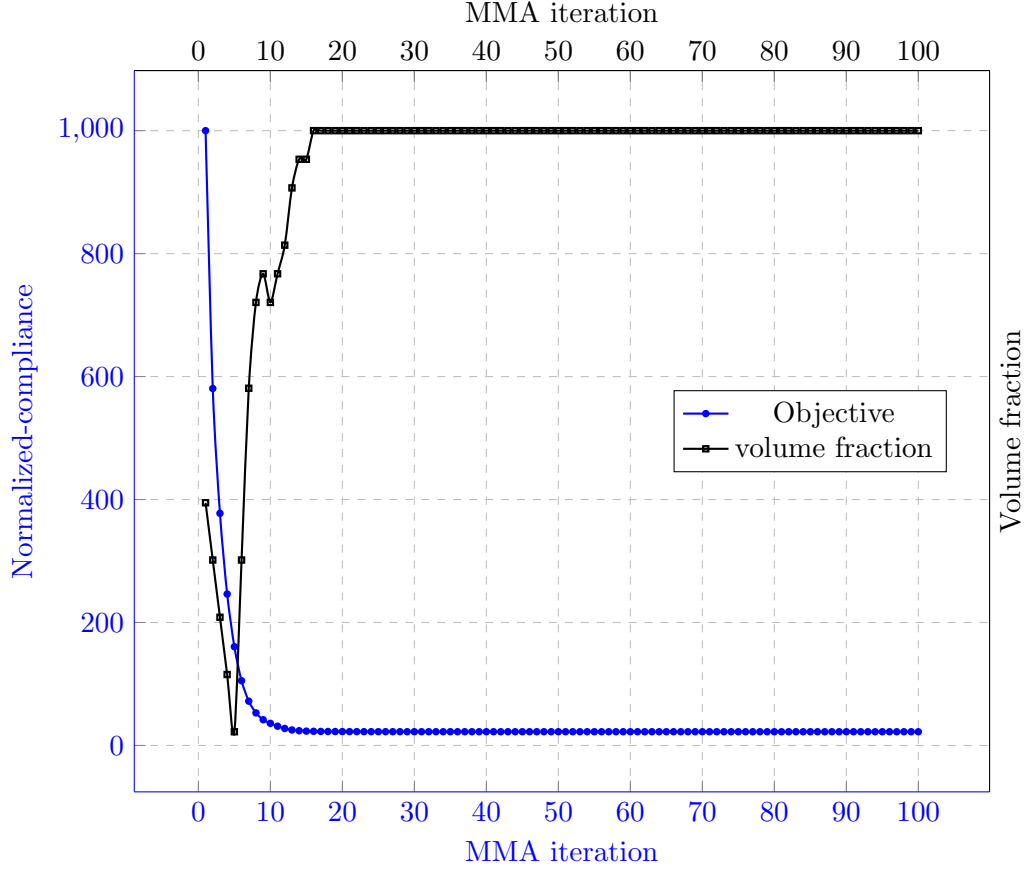


Figure 4: Convergence plot for the loadbearing lid structure

4.2 Externally Pressurized Structure

An externally pressurized structure is optimized. This particular problem is previously reported in Kumar and Langelaar (2021); Zhang et al. (2010); Du and Olhoff (2004). The design domain is depicted in Fig. 5. The top surface of the structure experiences a fluidic pressure load, while the left and right edges of the bottom face are fixed, as depicted in the figure. The left and right faces can slide in the z -direction. The bottom, back, and front faces get zero pressure loading. The dimensions of the domain are considered to be $2 \times 1 \times 1$. Note that the optimization is focused exclusively on the symmetry half of the domain for this case.

For applying the pressure load, line 90 is modified to

```
PF(unique([BTface, Fface, Bface]))= 0; PF(Tface) = Pin;
```

Boundary conditions are applied by replacing the lines 94-96 with the following code:

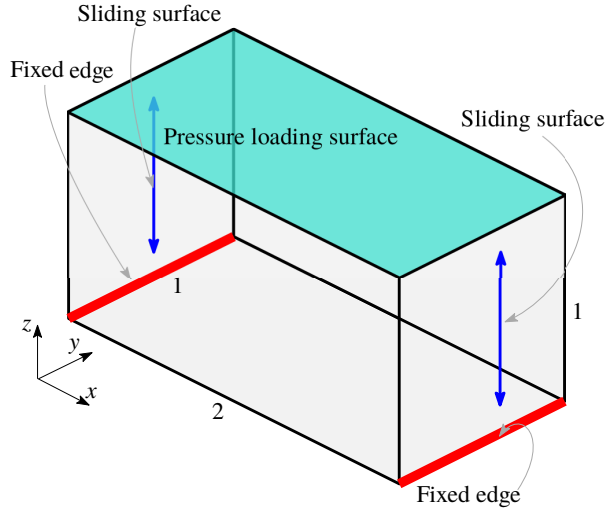
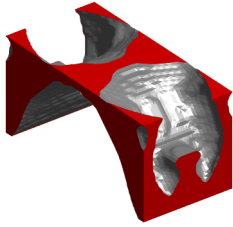
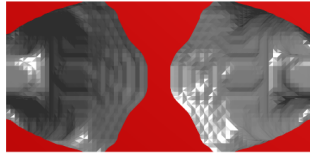


Figure 5: Design domain for an externally pressurized structure. The pressure load is applied on the top surface. The bottom, front and back faces get zero pressure loading. The left and right edges of the bottom face are fixed. The left and right faces slid in the vertical direction.



(a) Isoparametric view



(b) Top view



(c) Front view



(d) Front view

Figure 6: Optimized pressure loadbearing lid structure in different views. The symmetrical half domain is parameterized using $36 \times 36 \times 36$ FEs. The density value of the isosurface displayed is 0.3

```
fixnn = intersect(BTface,Rface);
fixedUdofs = [3*fixnn-2 3*fixnn-1 3*fixnn 3*Lface-2 3*Rface-1 3*Rface-2] ;
```

In the plotting routine, one replaces line 155 with the following code to plot the full optimized design from the symmetrical half result:

```
cla; isovals = zeros(nelx*2,nely,nelz);
isovals(nelx+1:2*nelx,1:nely,1:nelz) = shiftdim(reshape(xphys,nely,nelz,nelx),2);
isovals(1:nelx,1:nely,1:nelz) = isovals(2*nelx:-1:nelx+1,1:nely,1:nelz);
```

With the above modifications TOPress3D code is called as

```
TOPress3D(36,36,36,0.25,3,sqrt(3),0.2,10,1,100);
```

with $nelx = 36$, $nely = 36$, $nelz = 36$, $volf = 0.25$, $rmin = \sqrt{3}$, $etaf = 0.20$, $betaf = 10$, $lst = 1$, $maxit = 100$.

The optimized design with different views is illustrated in Fig. 6. The results are displayed with isosurface 0.3. The symmetrical half-optimized design is suitably converted into a full optimized design using the above plotting code. We find that convergences for the objective and volume constraint are smooth, and the volume constraint remains active at the end of the optimization.

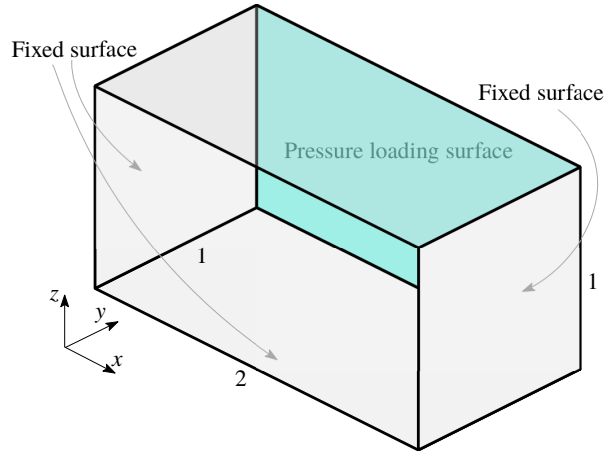


Figure 7: A Dam design domain. The bottom, left, and right faces are fixed. The back face experiences pressure load, whereas the front face receives no pressure load.

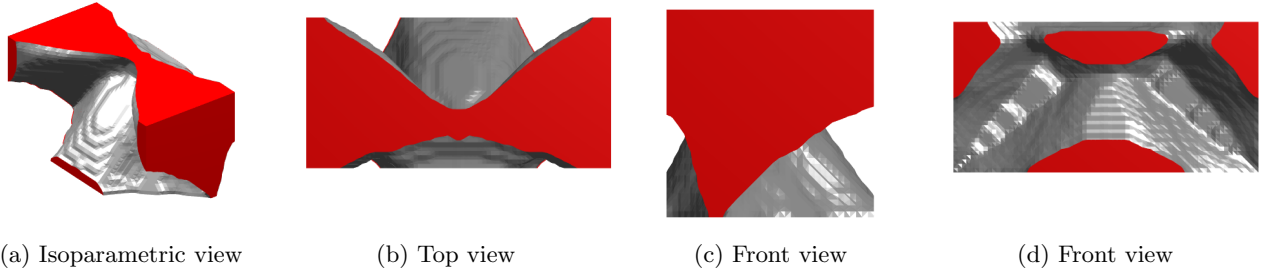


Figure 8: Optimized pressure loadbearing dam structure in different views. The symmetrical half domain is parameterized using $36 \times 36 \times 36$ FEs. The density value of the isosurface displayed is 0.3

4.3 Dam Structure

A dam structure, solved first in Sigmund and Clausen (2007), is optimized. The design domain is shown in Fig. 7. The pressure load is applied on the back face of the domain, whereas the front face experiences zero pressure load. The left, right, and bottom faces are fixed. Note that designing an actual damp structure requires complicated loading and boundary conditions (Sigmund and Clausen, 2007). The dimensions of the domain are $2 \times 1 \times 1$. Utilizing the symmetry of the problem, only one-half of the domain is optimized.

To solve this problem using `TOPress3D`, one modifies line 90 to

```
PF(Fface) = 0; PF(Bface) = Pin;
```

and line 94-96 to

```
fixnn = unique([BTface,Rface]);
fixedUdofs = [3*fixnn-2 3*fixnn-1 3*fixnn 3*Lface-2];
```

In the plotting, we perform a similar code presented for an externally pressurized structure. Having done the above modification, the user can call `TOPress3D` code as

```
TOPress3D(36,36,36,0.5,3,sqrt(3),0.2,10,1,100);
```

wherein $nelx = 36$, $nely = 36$, $nelz = 36$, $volf = 0.5$, $rmin = \sqrt{3}$, $etaf = 0.20$, $betaf = 10$, $lst = 1$, $maxit = 100$.

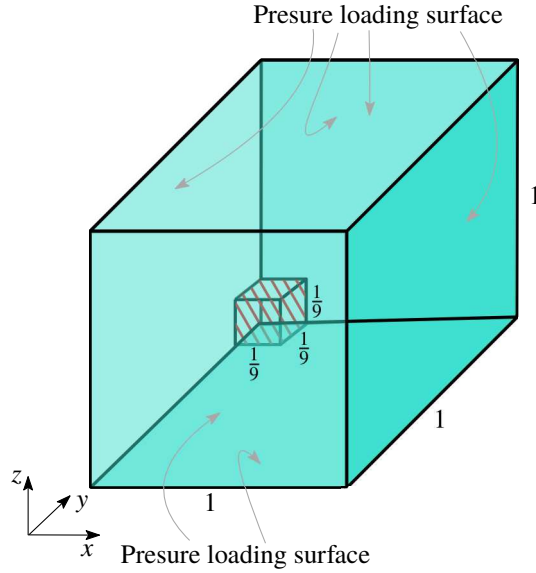


Figure 9: An externally pressurized hull structure. The structure is pressurized from all sides. A center cuboid void region is present, which is fixed.

The optimized design in the full domain is shown in Fig. 8. Different views are also depicted in the figure. The optimized design resembles that presented in Sigmund and Clausen (2007). The convergence of optimization's progress is found to be smooth.

4.4 Externally Pressurized hull structure

To demonstrate the code's capability with design domains having passive regions, we optimize a pressure hull structure herein (Wang and Qian, 2020). Fig. 9 depicts the design domain of the structure. All the surfaces are pressurized from the outside. The hull's center contains a cuboid passive void region, which is fixed (Fig. 9). The dimensions of the domain and void region are $1 \times 1 \times 1$ and $\frac{1}{9} \times \frac{1}{9} \times \frac{1}{9}$, respectively. Note that one may change the size of the void as per the requirement.

One makes the following modifications in `TOPress3D` to solve this problem. Line 86 is replaced by

```
elNrs = reshape(1:nel,nely, nelz, nelx);
v1 = elNrs(8*nely/18:10*nely/18,8*nelz/18:10*nelz/18,8*nelx/18:10*nelx/18);
[NDS, NDV] = deal( [],[v1(:)] );
Vnode = unique(Pdofs(v1(:),:));
```

where `elNrs` matrix arranges the element number in 3D matrix fashion using `reshape` MATLAB inbuilt function. `v1` extracts the information of FEs which are inside the void region (Fig. 9). Using `v1`, next, `NDV` is determined. Nodes constituting elements in `v1` are extracted in vector `Vnode` using matrix `Pdofs`. Now, to apply the pressure load, line 90 is changed to

```
PF(unique([BTface Bface Tface Fface Lface Rface])) = Pin; PF(Vnode(:)) = 0;
```

and boundary conditions are applied by changing lines 94-96 to

```
fixedUdofs = [ 3*Vnode(:)-2 3*Vnode(:)-1 3*Vnode(:)];
```

After performing the above modification, `TOPress3D` code is called as

```
TOPress3D(36,36,36,0.2,3,sqrt(3),0.2,10,1,100);
```

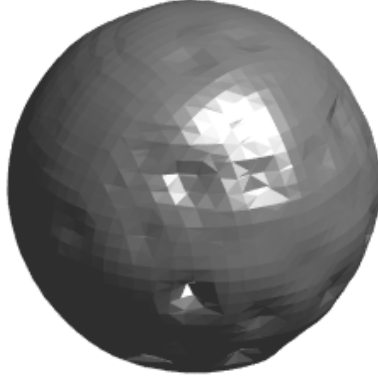


Figure 10: Optimized pressure loadbearing hull design.

with `nelx` = 36, `nely` = 36, `nelz` = 36, `volf` = 0.5, `rmin` = $\sqrt{3}$, `etaf` = 0.20, `betaf` = 10, `lst` = 1, `maxit` = 100.

The optimized pressure loadbearing hull structure is illustrated in Fig. 10. The optimized hull structure resembles that presented in Wang and Qian (2020). The objective and volume fraction convergence are smooth and have a convergence nature.

The working and success of the presented **TOPress3D** are demonstrated above in four examples. We envision that the code will allow people new to the topology optimization field to learn and explore different applications. The code can also be extended to solve pressure loadbearing structures with advanced constraints, e.g., stress constraints, buckling constraints, etc.

5 Concluding remarks

This paper introduces a MATLAB code, **TOPress3D**, comprising 160 lines, for 3D topology optimization for structures with design-dependent pressure loads. While such loads are encountered in various applications, addressing them within a TO framework proves challenging due to the dynamic nature of their magnitude, direction, and location during (especially at the beginning of) the optimization process. These challenges are particularly evident in 3D TO problems, potentially posing difficulties for newcomers and students on the learning path. The developed **TOPress3D** can become a valuable tool and practical gateway for individuals entering the field, including newcomers, students, and researchers. The code utilizes the method of moving asymptotes to update design variables. Darcy’s law with a drainage term is used to determine the pressure field in terms of the design values. The obtained pressure field is converted to consistent nodal loads.

The code (Appendix B) comprises six main subroutines, each explained in detail within the paper. Efficiency in matrix assembly is improved by representing mesh-related quantities as integers (MATLAB `int32`) and assembling only one half of the matrices. The transformation matrix is assembled before the optimization process, as its elemental part is independent of the design vector; which in turn saves computational time. To determine the state variables (pressure and displacement herein) one can also utilize the preconditioned iterative solvers as mentioned in **TOPress3D**.

The structure’s compliance is minimized with specified volume constraints. The efficacy and robustness of the code are demonstrated for designing four pressure loadbearing structures. **TOPress3D** is the default for optimizing the pressure loadbearing lid structure. The convergence plots for the objective and volume constraint are smooth. Extensions of the code are mentioned to solve different pressure loadbearing structures. We anticipate that the code will serve as a valuable platform for learning,

development, and extension to diverse applications involving design-dependent loads and opens several possibilities for future research.

Appendix A

Appendix B

References

- Kumar, P., Langelaar, M.: On topology optimization of design-dependent pressure-loaded three-dimensional structures and compliant mechanisms. *International Journal for Numerical Methods in Engineering* **122**(9), 2205–2220 (2021)
- Hammer, V.B., Olhoff, N.: Topology optimization of continuum structures subjected to pressure loading. *Structural and Multidisciplinary Optimization* **19**(2), 85–92 (2000)
- Kumar, P., Frouws, J.S., Langelaar, M.: Topology optimization of fluidic pressure-loaded structures and compliant mechanisms using the Darcy method. *Structural and Multidisciplinary Optimization* **61**(4), 1637–1655 (2020)
- Sigmund, O.: A 99 line topology optimization code written in matlab. *Structural and multidisciplinary optimization* **21**(2), 120–127 (2001)
- Amir, O., Aage, N., Lazarov, B.S.: On multigrid-CG for efficient topology optimization. *Structural and Multidisciplinary Optimization* **49**(5), 815–829 (2014)
- Liu, K., Tovar, A.: An efficient 3D topology optimization code written in matlab. *Structural and Multidisciplinary Optimization* **50**(6), 1175–1196 (2014)
- Saxena, A.: Topology design with negative masks using gradient search. *Structural and Multidisciplinary Optimization* **44**(5), 629–649 (2011)
- Kumar, P.: HoneyTop90: A 90-line MATLAB code for topology optimization using honeycomb tessellation. *Optimization and Engineering* **24**(2), 1433–1460 (2023)
- Talischí, C., Paulino, G.H., Pereira, A., Menezes, I.F.: PolyTop: a matlab implementation of a general topology optimization framework using unstructured polygonal finite element meshes. *Structural and Multidisciplinary Optimization* **45**(3), 329–357 (2012)
- Chi, H., Pereira, A., Menezes, I.F., Paulino, G.H.: Virtual element method (VEM)-based topology optimization: an integrated framework. *Structural and Multidisciplinary Optimization* **62**, 1089–1114 (2020)
- Singh, N., Kumar, P., Saxena, A.: Three-dimensional material mask overlay topology optimization approach with truncated octahedron elements. *Journal of Mechanical Design* **146**(1) (2024)
- Picelli, R., Neofytou, A., Kim, H.A.: Topology optimization for design-dependent hydrostatic pressure loading via the level-set method. *Structural and Multidisciplinary Optimization* **60**(4), 1313–1326 (2019)
- Du, J., Olhoff, N.: Topological optimization of continuum structures with design-dependent surface loading—part i: new computational approach for 2D problems. *Structural and Multidisciplinary Optimization* **27**(3), 151–165 (2004)

- Zhang, H., Liu, S.-T., Zhang, X.: Topology optimization of 3D structures with design-dependent loads. *Acta Mechanica Sinica* **26**(5), 767–775 (2010)
- Yang, X.-Y., Xie, Y.-M., Steven, G.: Evolutionary methods for topology optimisation of continuous structures with design dependent loads. *Computers & structures* **83**(12-13), 956–963 (2005)
- Sigmund, O., Clausen, P.M.: Topology optimization using a mixed formulation: an alternative way to solve pressure load problems. *Computer Methods in Applied Mechanics and Engineering* **196**(13-16), 1874–1889 (2007)
- Wang, C., Qian, X.: A density gradient approach to topology optimization under design-dependent boundary loading. *Journal of Computational Physics* **411**, 109398 (2020)
- Pinskier, J., Kumar, P., Langelaar, M., Howard, D.: Automated design of pneumatic soft grippers through design-dependent multi-material topology optimization. In: 2023 IEEE International Conference on Soft Robotics (RoboSoft), pp. 1–7 (2023). IEEE
- Pinskier, J., Wang, X., Liow, L., Xie, Y., Kumar, P., Langelaar, M., Howard, D.: Diversity-based topology optimization of soft robotic grippers. *Advanced Intelligent Systems*, 2300505 (2024)
- Wang, C., Zhao, Z., Zhou, M., Sigmund, O., Zhang, X.S.: A comprehensive review of educational articles on structural and multidisciplinary optimization. *Structural and Multidisciplinary Optimization* **64**(5), 2827–2880 (2021)
- Amir, O.: Revisiting approximate reanalysis in topology optimization: on the advantages of recycled preconditioning in a minimum weight procedure. *Structural and Multidisciplinary Optimization* **51**, 41–57 (2015)
- Aage, N., Andreassen, E., Lazarov, B.S.: Topology optimization using PETSc: An easy-to-use, fully parallel, open source topology optimization framework. *Structural and Multidisciplinary Optimization* **51**, 565–572 (2015)
- Lagaros, N.D., Vasileiou, N., Kazakis, G.: AC# code for solving 3D topology optimization problems using sap2000. *Optimization and Engineering* **20**, 1–35 (2019)
- Ferrari, F., Sigmund, O.: A new generation 99 line matlab code for compliance topology optimization and its extension to 3D. *Structural and Multidisciplinary Optimization* **62**(4), 2211–2228 (2020)
- Schmidt, S., Schulz, V.: A 2589 line topology optimization code written for the graphics card. *Computing and Visualization in Science* **14**, 249–256 (2011)
- Deng, H., Vulimiri, P.S., To, A.C.: An efficient 146-line 3D sensitivity analysis code of stress-based topology optimization written in MATLAB. *Optimization and Engineering*, 1–29 (2021)
- Zuo, Z.H., Xie, Y.M.: A simple and compact Python code for complex 3D topology optimization. *Advances in Engineering Software* **85**, 1–11 (2015)
- Fernández, E., Collet, M., Alarcón, P., Bauduin, S., Duysinx, P.: An aggregation strategy of maximum size constraints in density-based topology optimization. *Structural and Multidisciplinary Optimization* **60**, 2113–2130 (2019)
- Smith, H., Norato, J.A.: A MATLAB code for topology optimization using the geometry projection method. *Structural and Multidisciplinary Optimization* **62**(3), 1579–1594 (2020)
- Wang, Y., Kang, Z.: MATLAB implementations of velocity field level set method for topology optimization: an 80-line code for 2D and a 100-line code for 3D problems. *Structural and Multidisciplinary Optimization* **64**(6), 4325–4342 (2021)

- Du, Z., Cui, T., Liu, C., Zhang, W., Guo, Y., Guo, X.: An efficient and easy-to-extend matlab code of the Moving Morphable Component (MMC) method for three-dimensional topology optimization. *Structural and Multidisciplinary Optimization* **65**(5), 158 (2022)
- Zhao, Y., Guo, G., Zuo, W.: Matlab implementations for 3D geometrically nonlinear topology optimization: 230-line code for SIMP method and 280-line code for MMB method. *Structural and Multidisciplinary Optimization* **66**(7), 146 (2023)
- Zhuang, C., Xiong, Z., Ding, H.: An efficient 2D/3D NURBS-based topology optimization implementation using page-wise matrix operation in MATLAB. *Structural and Multidisciplinary Optimization* **66**(12), 1–23 (2023)
- Kim, D., Ji, Y., Lee, J., Yoo, J., Min, S., Jang, I.G.: A MATLAB code of node-based topology optimization in 3D arbitrary domain for additive manufacturing. *Structural and Multidisciplinary Optimization* **65**(11), 311 (2022)
- Kumar, P.: TOPress: a MATLAB implementation for topology optimization of structures subjected to design-dependent pressure loads. *Structural and Multidisciplinary Optimization* **66**(4) (2023)
- Svanberg, K.: The method of moving asymptotes—a new method for structural optimization. *Int J Numer Meth Eng* **24**(2), 359–373 (1987)
- Kumar, P., Langelaar, M.: Topological synthesis of fluidic pressure-actuated robust compliant mechanisms. *Mechanism and Machine Theory* **174**, 104871 (2022)
- Kumar, P.: Towards Topology Optimization of Pressure-Driven Soft Robots. In: *Conference on Microactuators and Micromechanisms*, pp. 19–30 (2022). Springer
- Kumar, P., Saxena, A.: An improved material mask overlay strategy for the desired discreteness of pressure-loaded optimized topologies. *Structural and Multidisciplinary Optimization* **65**(10), 304 (2022)
- Banh, T.T., Shin, S., Kang, J., Lee, D.: Frequency-constrained topology optimization in incompressible multi-material systems under design-dependent loads. *Thin-Walled Structures* **196**, 111467 (2024)
- Kumar, P.: Topology optimization of pressure-loaded multi-material structures. In: *Advances in Structural Integrity for Mechanical, Civil, and Aerospace Applications* (2024 (accepted)). Springer
- Bruns, T.E., Tortorelli, D.A.: Topology optimization of non-linear elastic structures and compliant mechanisms. *Comput Method Appl Mech Eng* **190**(26-27), 3443–3459 (2001)
- Kumar, P.: SoRoTop: a hitchhiker’s guide to topology optimization MATLAB code for design-dependent pneumatic-driven soft robots. *Optimization and Engineering*, 1–35 (2024)
- Engblom, S., Lukarski, D.: Fast matlab compatible sparse assembly on multicore computers. *Parallel Computing* **56**, 1–17 (2016)
- Zienkiewicz, O.C., Taylor, R.L., Zhu, J.Z.: *The Finite Element Method: Its Basis and Fundamentals*. Elsevier, Butterworth-Heinemann (2005)